

## Application of Remote Sensing for Geological Mapping Using Landsat etm+ Satellite image For Part of Western Hazara Ranges Across Siran River, North Pakistan

Muhammad Qasim<sup>1,2,3\*</sup> Muhammad Asif Khan<sup>3,4</sup> Muhammad Haneef<sup>2</sup>, Qasim-Ur-Rehman<sup>5</sup>,  
Muhammad Qaiser Khan<sup>6</sup>, Muhammad Nakir Shah<sup>6</sup>

<sup>1</sup> Institute of Tibetan Plateau Research, CAS, Beijing, China

<sup>2</sup> Department of Earth Sciences, COMSATS IIT, Abbottabad, Pakistan

<sup>3</sup> NCE in Geology, University of Peshawar.

<sup>4</sup> Karakorum International University, Gilgit.

<sup>5</sup> Department of Geology, University of Haripur.

<sup>6</sup> Geological Survey of Pakistan, 84, H-8/1, Islamabad

\*(Corresponding author Email: qasimtanoli@cuiatd.edu.pk)

### ABSTRACT

The Aluli area, Western Hazara Ranges, comprises of Precambrian Tanawal Formation, Early Cambrian Abbottabad Formation and Recent alluvium. These formations consist of variety of lithological units including phyllite, quartzites, quartz mica schist, sandstones, siltstones, conglomerates, dolomites, limestones and alluvium. The geological mapping of these constituent lithologies is carried out using Landsat Enhanced Thematic Mapper Plus (ETM+) image enhancement techniques, which include band composition and band rationing. The False Color Composite (FCC) 5-3-1 is found significant to recognize the folds and faults on LandsatETM+ satellite image. The FCCs 7-5-4, 4-5-7 and 3/1-5/7-5/4 are best in differentiating the geological units. The field mapping along selected traverses gave a better control to identify the specific lithological units on the FCC images. This exercise gives a better geological control to extend the geological units to nearby areas. This study provides a

simple supplementary and effective application of Landsat ETM+ satellite image to be used in the future as an aid to geological mapping.

**Keywords:** Remote Sensing, Landsat ETM+, Geological Mapping, Hazara Ranges, Band Composition, Band Rationing.

### 1. INTRODUCTION

One of the fundamental objectives of geological studies is classification of rocks into units (based on their lithological characteristics and ages) and determining their interrelationship. For this geologist use their observations in combination of their expert knowledge to develop geological maps. Normally geological maps are based on topographic maps, such as geological maps of the Geological Survey of Pakistan are based on Survey of Pakistan topographic maps. However, aerial photographs have also been extensively used as base maps as well as an aid in distinguishing various rock units

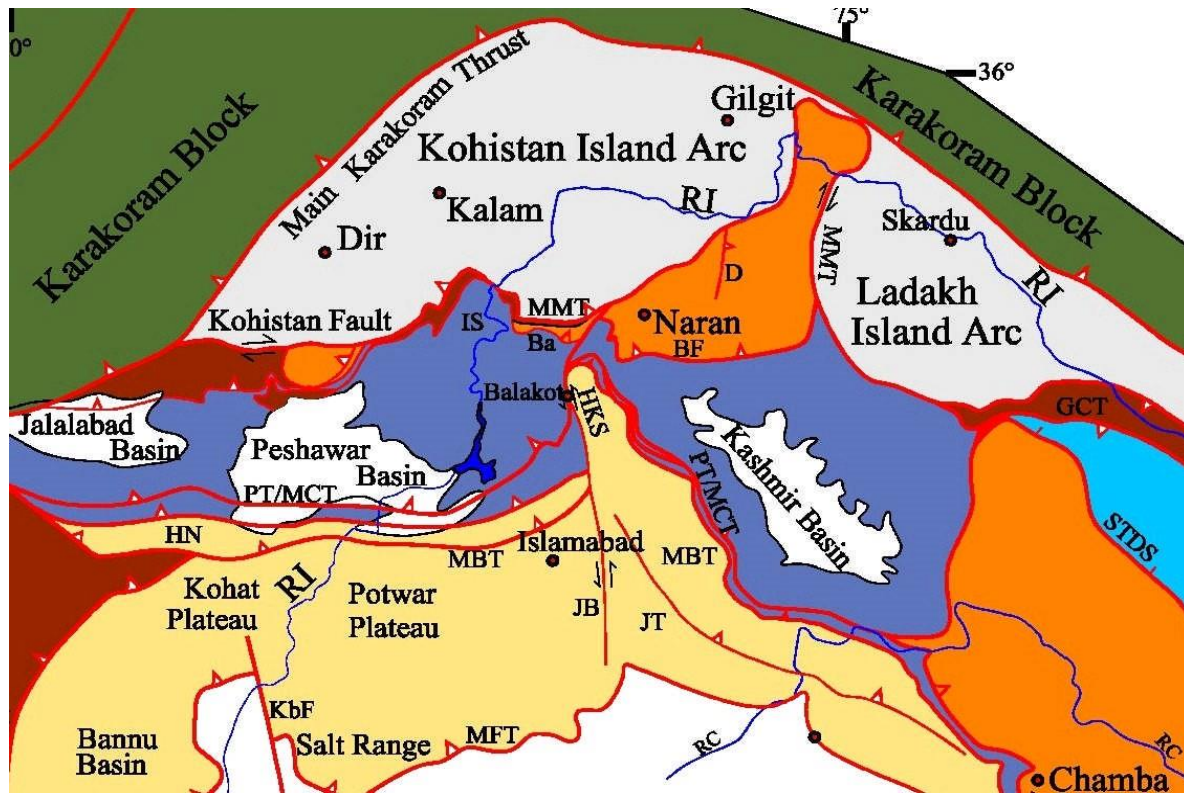


Figure 1 - Tectonic Map of Western Himalaya showing major tectonic divisions and structures. The black filled rectangle indicates the study area. MFT-Main Frontal Thrust (Salt Range Thrust), MBT-Main Boundary Thrust (Murree Thrust), MCT-Main Central Thrust, PT-Panjal Thrust, HN-Hissartang-Nathia Gali Thrust, IS-Indus Syntaxis, Ba-Banna Fault, GCT-Great Counter Thrust, MT-Main Mantle Thrust, STDS-South Tibetan Detachment System, JB-Jhelum Balakot Fault, B-Batal Fault, D-Diamir Fault, JT-Jammu Thrust, RI-River Indus, RC- River Chenab, Ab-Abbottabad, Sh-Sherwan (This Figure is based on many sources and modified after DiPietro and Pogue (2004).

(Eardley, 1942; Ferrero et al., 2009; Ferrero et al., 2011; Jones, 1961; Kottenstette, 2005, Latif, 1970; MORRIS, 1964; Paine and Kiser, 2012).

With the advent of satellite-based remote sensing since 1970s (such as (ERTS) Landsat series), geologists have been provided a new powerful tool to aid them in geological mapping. Landsat multispectral scanner (MSS) with very near infrared (VNIR) bands was used to distinguish lithologies with different iron-oxide contents as early as 1980s (Dogan, 2008; Goetz and Rowan, 1981; Rawashdeh et al., 2006; Sabins,

1999). Higher spatial resolution furnished by French Satellite Pour l'Observation de la Terre (SPOT) system was extensively exploited for geological mapping, both for distinguishing the lithologies (Bilotti et al., 2000) as well as delineation of faults (Kavak, 2005; Kavak and Inan, 2002; Kaya et al., 2004). Currently, the Advanced Spaceborne Thermal Emission and Reflectance Radiometer, ASTER (Abrams, 2000; Mars and Rowan, 2010; Rajendran et al., 2011; Yamaguchi et al., 1998) has provided better mineral mapping capabilities for the remote sensing geologists. Subsequently, remote-sensing sensors such

as Landsat Thematic Mapper (TM) and Enhanced Thematic Mapper (ETM) with access to 6 and 7 bands data, respectively (as opposed to 3 bands data by SPOT) became popular in geology (Gad and Kusky, 2006; Schetselaar et al., 2000; Yazdi et al., 2013). Several techniques have been developed to process the satellite images such as band rationing, decorrelation stretching and saturation enhancement and Principal Component Analysis (PCA) (Chavez et al., 1991; Yesou et al., 1993), which has been effectively used to develop lithological contrasts to map the contacts and delineation of fault lineaments.

Besides spectral mapping, the geological interpretation of satellite images added considerable knowledge of the geology of less explored parts of the world (Bannert et al., 1993).

Since the primary objective of the present study is geological mapping with aims at investigating stratigraphic and structural relations between the constituent lithological units in study area (Figure 1), satellite remote sensing has been applied as an aid in 1) distinction between lithologies, and 2) delineation of structural features such as folds and faults. The Landsat Enhanced Thematic Mapper Plus (ETM+) satellite image is used for the interpretation of geological structures and lithologies. The Landsat ETM+ image has been processed using techniques such as band composition and band rationing (Figure 2). The Landsat ETM+ satellite image scene used for this study is 150/36 (Acquisition date is 07, October, 2001) with 30 m spatial resolution. The interpretation of the geological units on

satellite images was supplemented with field mapping along selected traverses (Figure 1). This integrated approach resulted in the development of geological and structural map of the study area at a scale of 1:50000 (Figure 3).

## **2. STUDY AREA AND GEOLOGICAL SETTING**

The western Hazara ranges, subject of this study, are a part of the Western Himalayas that cover Hazara and Swat regions of northern Pakistan. In the east, Hazara-Kashmir syntaxis separated these ranges from Kashmir Himalayas (Bossart et al., 1988; Wadia, 1931). Hazara-Kashmir syntaxis is a pivotal point where the major orographic trends of the Kashmir Himalaya change. In the west, another antiformal structure termed Indus Syntaxis, separate the Hazara ranges from Swat Ranges (DiPietro and Pogue, 2004) (Figure 1). Unlike the Hazara and Swat regions, much of the Peshawar basin and mountain ranges to the south are devoid of involvement in the Indus syntaxis, as shown by the continuation of the orographic trends in the Ghandghar-Attock-Cherat Ranges across the Indus River (Figure 1).

## **3. METHODOLOGY**

The methodology involved in preparation of revised geological map of western Hazara ranges consist of detailed field work and remote sensing. An area measuring 140 km<sup>2</sup> was mapped at 1:50,000 scale (Figure 3).

infrared (NIR) band, two short-wave infrared (SWIR) bands, 1 thermal infrared (TIR) band

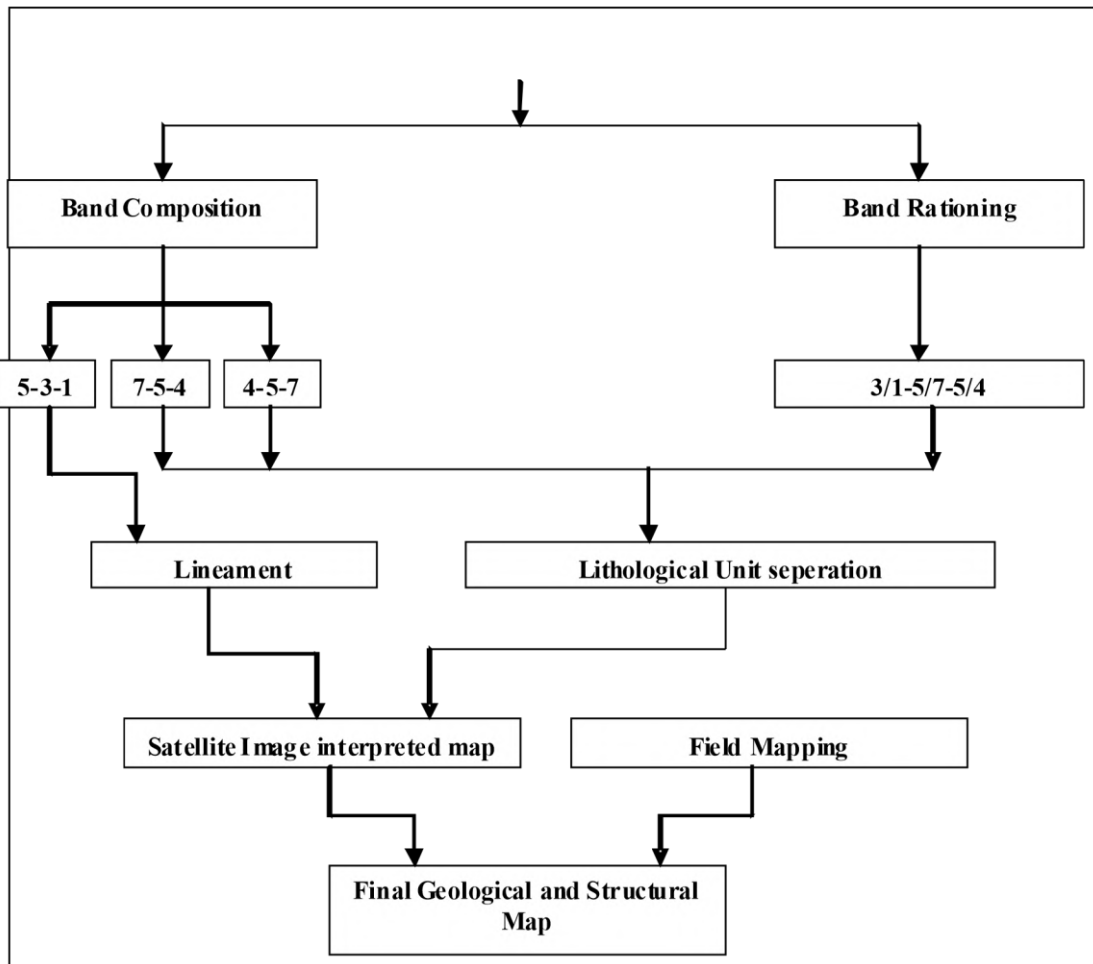


Figure. 2. Schematic diagram showing the image analysis techniques applied on Landsat

ETM+ satellite images

with 60 m resolution and 1 panchromatic band with a 15 m spatial resolution. Landsat ETM+ satellite image was processed through band composition and band rationing techniques to enhance contrast between constituent lithologies to map the contacts as well as large-scale fold and fault structures.

## 4. RESULTS

### 4.1. Geological mapping

The preparation of revised geological map for the part of western Hazara ranges between Aluli in the south and Bir in the

north is achieved through an extensive field work (Qasim et al., 2014; Qasim et al., 2015). The lithological contact and geological structures were mapped through number of traverses along roads and stream cuts (Figure 3). This strip mapping fashion gives a control to extend the geological contact between the mapped traverses.

### Stratigraphy

The lithostratigraphy mapped in the study area consists of Precambrian Tanawal Formation, Early Cambrian Abbottabad



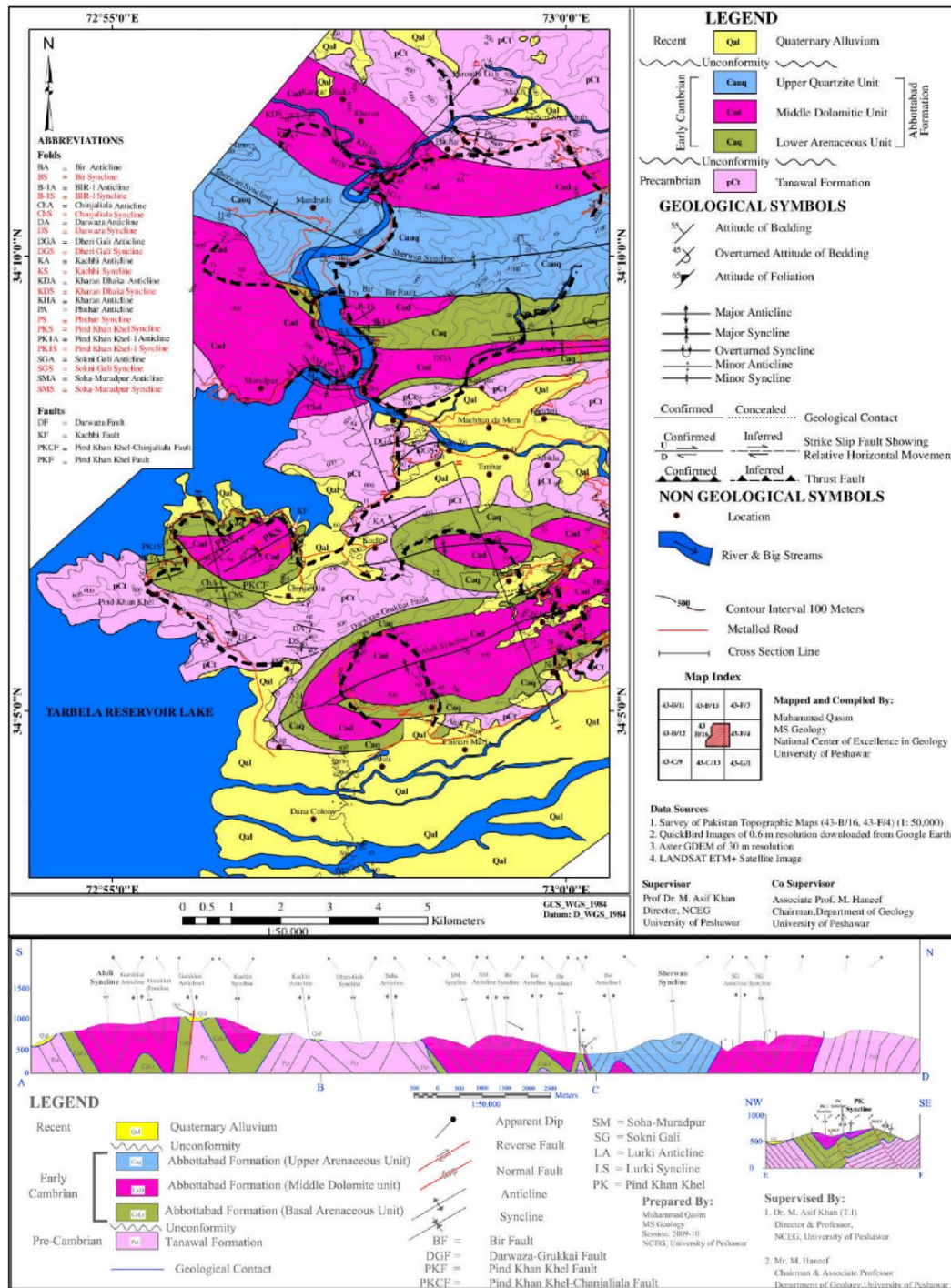


Figure -3 Geological and Structural map of the Western Hazara Ranges across Siran River, north Pakistan (Qasim et al., 2015). The dashed black bold line shows the field traverses for geological mapping. The structural cross-sections across the line ABCD and EF portraying structural geometry.

Formation and Quaternary Alluvium. The Abbottabad Formation in study area is further divided into three members;

- 1) Lower arenaceous unit,
- 2) Intermediate dolomite unit, and
- 3) Upper Quartzite unit (Qasim et al., 2014).

The Tanawal Formation comprises of quartzite, quartzose sandstone, argillaceous sandstone, phyllite, shale, and quartzose conglomerate (Table 1). Quartzite and sandstone are thick to massive in bedding. The dolerite dykes and sills are common in the sequence. The contact of the Tanawal Formation with overlying Abbottabad Formation is

Table 1. Simplified Stratigraphic column of the studied area showing lithological units

Log	Present Study	Lithological Description	Age
	Upper Quartzite Unit	Quartzite, fine grained to sub-conglomeratic	Early Cambrian
	Middle Dolomitic Unit	Dolomite with quartzite, siltstone and conglomerates	
	Lower Arenaceous Unit	conglomerates, quartz mica schist, quartzite, sandstones and siltstones	
	Tanawal Formation	Dominantly quartzite, quartzose sandstone and schist	Precambrian

unconformable and marked by the presence of conglomeratic bed.

The Abbottabad Formation consists of variety of lithologies including conglomerate, quartzite, sandstones.

### Structural Geology

Structurally, the project area is divided into three major fold structures (synclines), which are 1) Sherwan fold structure, 2) Aluli fold structure, and 3) Pind Khan Khel fold structure. These three-fold structures are synclinal folds comprising of syncline-anticline pairs developed on their limbs (Qasim et al., 2015). The core of these major fold structures is occupied by Cambrian Abbottabad Formation. The Sherwan fold structure in the north consists of 15 syncline-anticline pairs, which include Phuhar syncline-anticline pair comprised of Tanawal Formation, Sokni Gali syncline-anticline pair, Kharan anticline, Kangar Dhaka syncline-anticline pair. Sherwan Syncline is the central syncline of Sherwan fold structure. Bir syncline-anticline pair, Bir-1 syncline-anticline pair, Soha Muradpur syncline-anticline pair and Dheri-Gali syncline anticline pair. The southern limb is faulted along Bir fault (Figure 3). The Aluli fold structure covers the southern limits of the mapped area and extend northeastward beyond the project area (Figure 3). It consists of 6 syncline-anticline pairs which are Gruakkai syncline-anticline pair, Darwaza syncline anticline pair and Kachhi syncline-anticline pair. The northern limb of Aluli syncline is faulted along Aluli fault, while southern limb is faulted along Darwaza-Gruakkai Fault.

The Pind Khan Khel syncline consists of 4 syncline-anticline pairs, which are Chanjaliala syncline-anticline pair and

Pind Khan Khel-1 syncline-anticline pair.

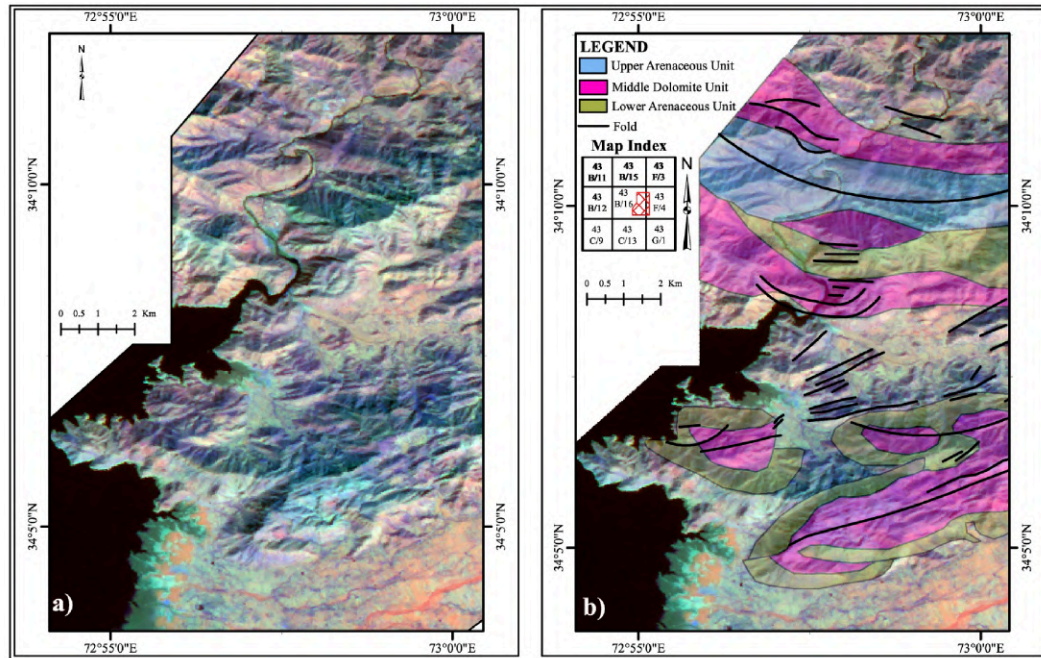


Figure 4 -LANDSAT ETM+ satellite images of FCC 7-5-4 showing geological units. a) FCC 7-5-4 un- interpreted image, b) FCC 7-5-4 interpreted image.

The Pind Khan Khel syncline is a faulted syncline (Figure 3).

The main faults are Aluli Fault, Bir Fault, Darwaza Fault, Darwaza-Grukkai Fault, Pind Khan Khel-Chanjaliala Fault and Pind Khan Khel Fault. These faults are transpressional in nature (Qasim et al., 2015).

#### 4.2. Satellite Image Analysis

Remote sensing based geological mapping is most effective when supplemented with field checks. Since, this study did not rely only on satellite remote-sensing data and carried out an extensive field mapping exercise interactively with satellite-remote sensing image analysis, the resulting

geological map has greater authenticity (Figure 3).

The Landsat ETM+ satellite images consist of six non thermal bands within a wavelength range of 0.4-0.25 micrometer. The Landsat ETM+ bands 1, 2, 3, 4, 5 and 7 consider to be most effective for geological discrimination as a three-band color composite (Ali and Pirasteh, 2004; Beauchemin and Fung, 2001). The band 4 produce high reflectance for limestone and dolomite due to the strong absorption between Landsat ETM+ bands 5 and 7 (Clark et al., 1990; Gaffey, 1986; Hunt and Salisbury, 1971). Thus, the resultant False Color Composite (FCC) displays the colors in shades of blue for the rocks containing carbonate minerals. The



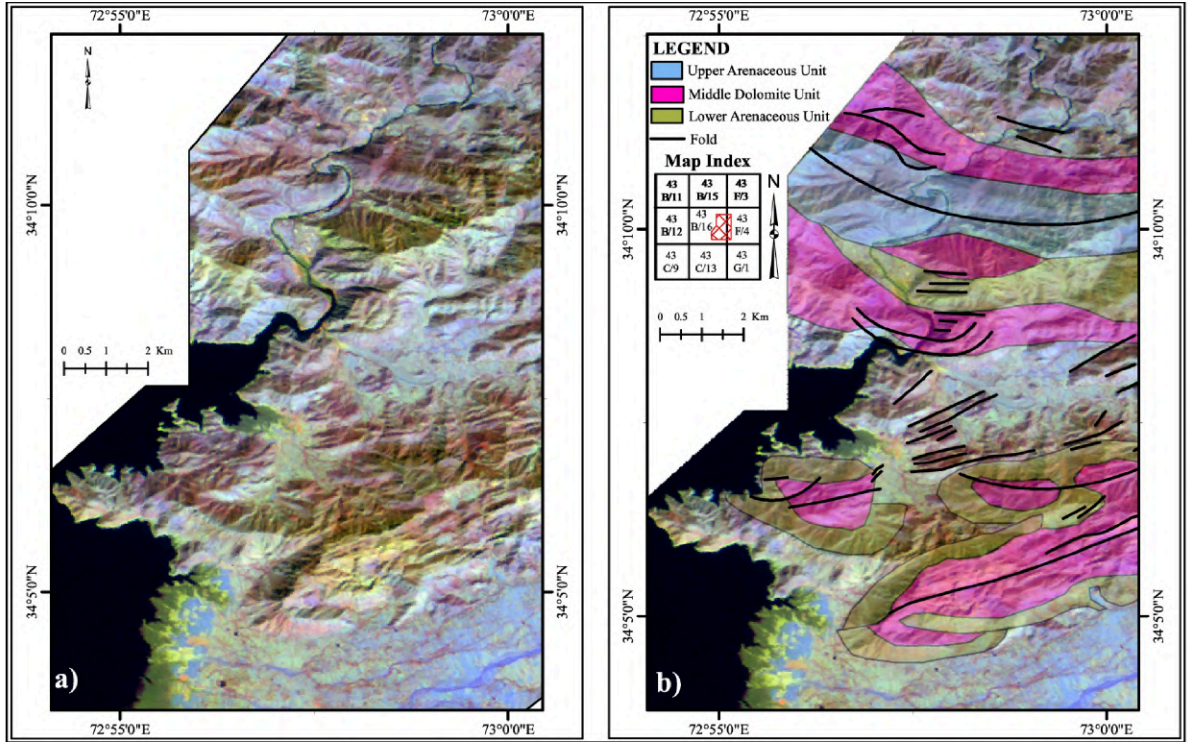


Figure 5 - LANDSAT ETM+ satellite images of FCC 4-5-7 showing geological units. a) FCC 4-5-7 un-interpreted image, b) FCC 4-5-7 interpreted image.

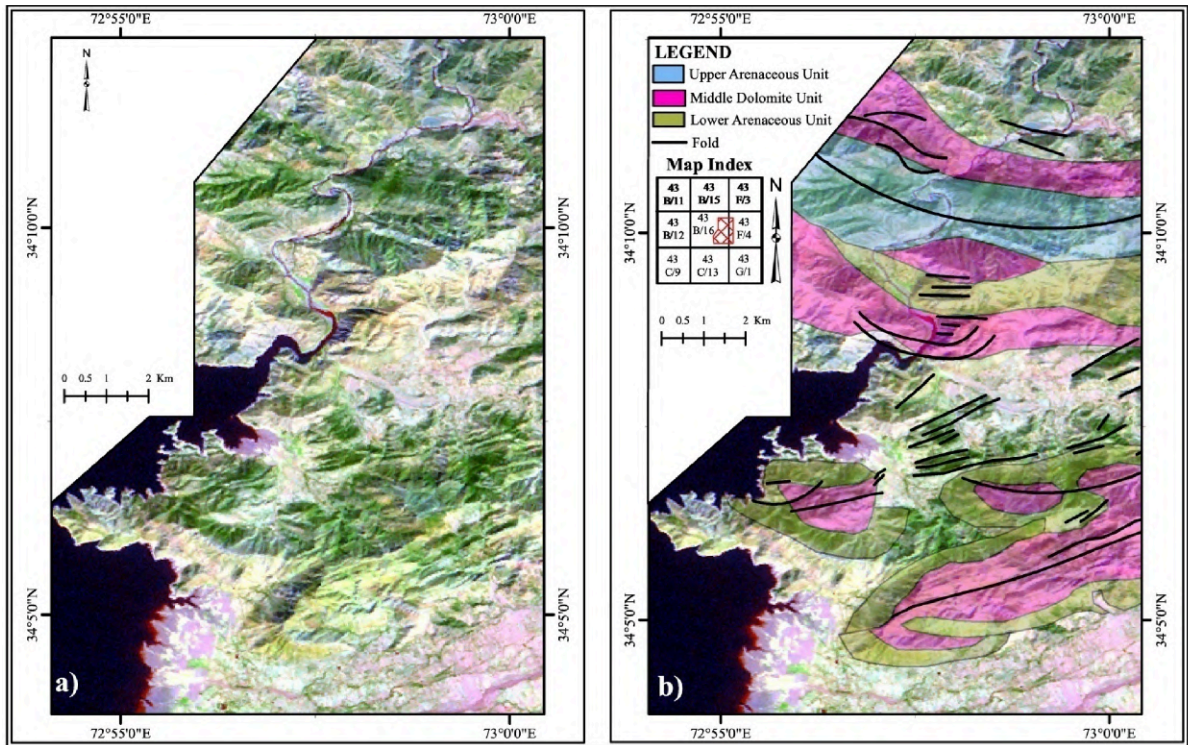


Figure 6 - Landsat ETM+ image with FCC of band ratios 3/1-5/7-5/4 showing different geological units and folds. a) Un-interpreted and b) Interpreted images.



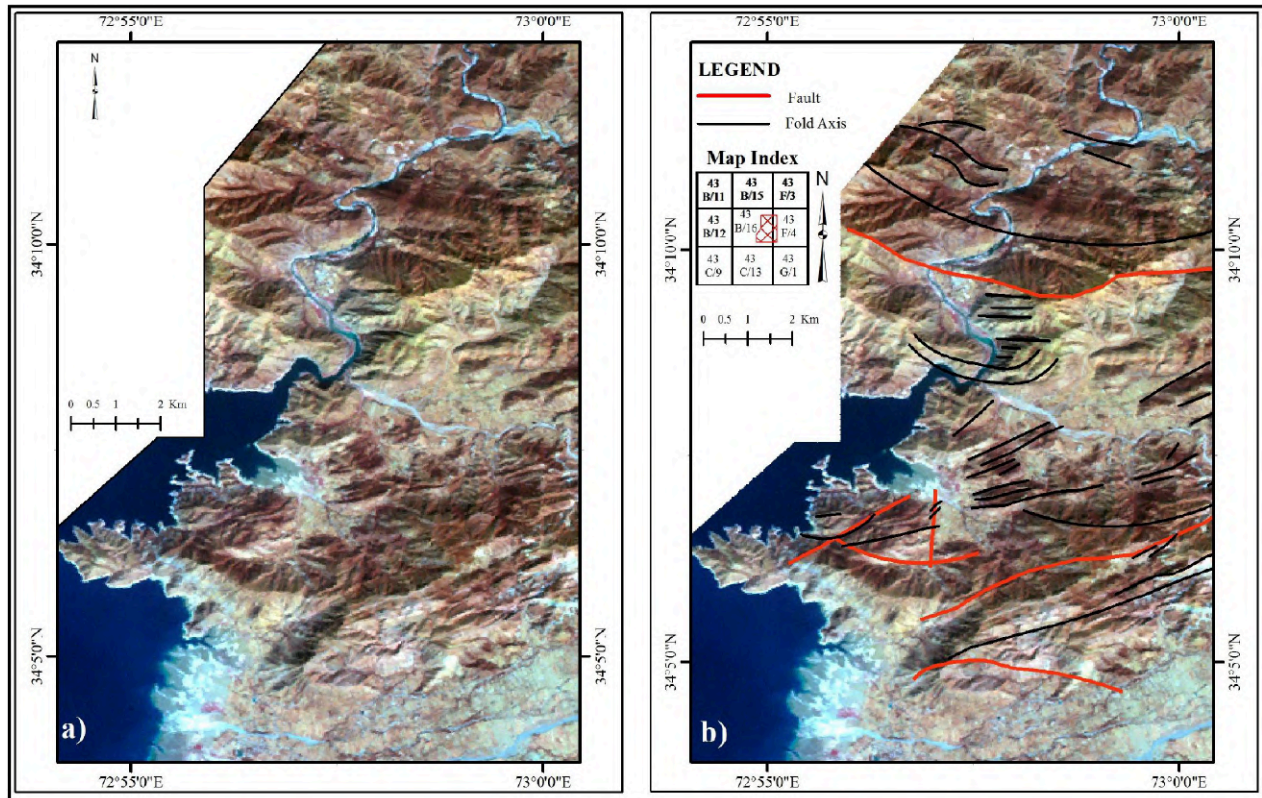


Figure 7 - Landsat ETM+ satellite images of FCC 5-3-1 a) Un-interpreted b) Interpreted showing faults and folds.

common mineral in the sedimentary rock is quartz, which usually display in white or grey color in FCC if not weathered. The presence of iron oxide in less weight percent also affects the reflectance of rock unit. Such as, sandstone generally has less than two weight percent of iron oxide exhibits a variety of color variation ranging from brown, yellow, and orange to red in FCC. Similarly, the rocks consisting of shale and micaceous minerals such as muscovite or biotite depict generally green color on FCC images due to high reflectance in band 4

as compared to band 7 and 1(Clark, 1999).

The presently studied area comprises of dominantly quartzite, phyllites, limestone and dolomites with substantial amount of sandstones (Qasim et al., 2014). Presently, we adopted the band composition of bands 7, 5, 4 and band ratios 3/1, 5/7, 5/4 for the geological differentiation of stratigraphic units. The individual lithologies and regional structures can be identified better on FCC images as compared to true color composite. The shadow of the mountains

or clouds may also hinder geological information in the satellite images. The careful examination of the pattern, texture and shape may help to differentiate the shadow and dark tone lithologies. However, the provision of the high-resolution Google Earth images also provide help in interpretation. In this study, the field work provided additional knowledge about the physical appearance of the different lithological units exposed in the study area. This provides greater help in the interpretation of the lithological units in the unmapped area.

### **Band Composition**

The band composition is a technique in which different electromagnetic radiation bands are combined in RGB (Red-Green-Blue) environment to enhance the difference in color contrast among different geological units. The band composition 3-2-1 is a true color composite that displays the natural color of the rocks and materials (Vincent, 1997). For the purpose of geological unit separation, the false color composite (FCC) of bands combination 7-5-4 and 4-5-7 have been used in a RGB environment in ARCGIS 10 in this study. In the FCC 7-5-4, the dolomite of the Abbottabad Formation is represented by light bluish to light greenish color; quartzite and sandstone by bluish to light purplish color and the quartzite of the Tanawal Formation yields purplish color (Figure 4). In the FCC 4-5-7, the dolomite of the Abbottabad Formation gives golden color, while the quartzite

yields light maroon color and quaternary alluvium, clay and stream channel deposits are represented by bluish grey color (Figure 5).

### **Band Rationing**

Band rationing is a method that has been applied in remote sensing for many years to efficiently exhibit spectral variations (Dehnavi et al., 2010). A ratio is created by the division of brightness values, pixel by pixel, of one band by another. The prime objective of these ratios is to improve the contrast between different materials by division of brightness values at peaks and cores in a spectral reflectance curve (Imbroane et al., 2007). This tends to improve spectral differences and suppress illumination differences. The band ratio of Landsat ETM+ satellite images are used to enhance rock alteration. The false color composite is then made in RGB environment.

The band ratios of Landsat ETM+ image is created in Envi 4.7 software for the project area. The band ratios 3/1, 5/7 and 5/4 are selected for separation of geological units. This combination is selected because it is sensitive to lithologic variables and lack of statistical redundancy (Crippen et al., 1990). The band ratio 3/1 enhances rocks containing limonite, for the hydro-thermal alteration or the oxidation of Fe-Mg silicates. The band ratio 5/7 enhances rocks containing AlOH, such as clay and sulphate minerals produced from hydrothermal fluids and associated with porphyry copper deposits and vegetation (Imbroane et al.,

2007). The bands ratio 5/4 enhances rocks that contain ferrous iron.

The FCC 3/1-5/7-5/4 application to the studied area displays the dolomite in light yellowish color, quartzite and sandstone in light green color and the quaternary alluvium, stream channel deposits in light pink color (Figure 6).

### **4.3. Faults and Folds**

The recognition of the folds and faults on the satellite image is based on topographic breaks, vegetation linearity, landscapes, tonal changes on the images, changes in drainage pattern with direction and discontinuity in the same lithology. (Ali and Pirasteh, 2004). The faults are recognized on the Landsat ETM+ image using false color composite combination of bands 5-3-1 (Figure 7). The folds and faults were traced on the satellite image in ARCGIS 10. The folds and faults are mapped along the field traverses in the study area (Figure 3). The trace of the fold axes and faults are extended on the satellite image to the unmapped area.

The field control enhanced the visual interpretation of the linear structures on the Landsat ETM+ satellite images. The folds and faults are recognized by red color and low color in the satellite images (Figure 7). The field mapping results greatly helped to trace the continuity of the linear structures on the satellite images. However, in this study the field traverses cover all the structures. Therefore, simple FCC is used to extend the linear structures. In the future, the available high resolution satellite images can be used for mapping of linear structures with

more advanced satellite image analyses in the areas where field control is limited.

### **5. Summary**

The study area being part of the western Himalaya is highly deformed into numerous folds and faults. The geology of the area comprises of Precambrian basement Tanawal Formation and Early Cambrian cover sequence of Abbottabad Formation. The mountainous terrain of the study area also covered in some places by dense vegetation, which creates hurdles in identification of lithologic units on the satellite image. However, present study in the western Hazara ranges, first time applied a satellite remote sensing technique as an aid for geological mapping together with the field work. The separation of the lithological units was possible by applying different numeric treatments. The FCC images obtained with combination of different band sets available in the Landsat ETM+ satellite image (Figures 4, 5, 6 and 7) have been used and found effective in identifying and separation of various lithological units. The image analysis techniques applied in this study include band composition and band rationing. The band composition of bands 7-5-4 and 4-5-7 are found suitable for differentiating lithological units in Aluli area due to a distinguishable color contrast. The high reflectance of limestone and dolomite in Landsat ETM+ band 4 gave shades of blue in a FCC 754. The presence of limestone and dolomites in the core of the Aluli syncline as mapped in the field traverses confirms the extension of the units to the unmapped area based on image interpretation. The combination of band



ratios used in this study is 3/1-5/7-5/4, and is found significant in the identification of lithological units. However, these results of satellite image analysis are later verified by the aid of field mapping to develop a composite geological map of the study area (see also Iqbal et al. PJHR 1998). This practice of combination of field work and satellite image analysis in the Aluli area seems effective and useful for the geological mapping.

We suggest, this practice should be applied to the remote areas in the future with more advanced image analysis techniques and high-resolution satellite data to constrain better mapping results.

## 6. CONCLUSION

The present study is a test case in the Aluli area, western Hazara ranges, northern Pakistan, which allowed us to apply different satellite image analysis techniques on Landsat ETM+ satellite image for differentiating the lithological units and also to carry out geological mapping. The results have been verified by fieldwork. This combination of fieldwork and satellite image analysis resulted in preparation of Geological and structural map on a scale of 1:50000. FCCs (7-5-4 and 4-5-7) and band rationing (3/1-5/7-5/4) provide excellent contrast to differentiate among different lithological units.

## Acknowledgement

This study was sponsored by the graduate student support program of the National Centre of Excellence in Geology, University of Peshawar. I am thankful to Mrs. Annette Lisy

of BGR (Project Manager, Geohazard Assessment Project Northern Pakistan) for allowing me to use the licensed version of ENVI and ArcGIS at Geological Survey of Pakistan, H-8/1.

## REFERENCES

- Abrams, M., 2000. The Advanced Spaceborne Thermal Emission and Reflection Radiometer (ASTER): data products for the high spatial resolution imager on NASA's Terra platform. *International Journal of Remote Sensing* 21,847-859.
- Ali, S.A., Pirasteh, S., 2004. Geological applications of Landsat Enhanced Thematic Mapper (ETM) data and Geographic Information System (GIS): Mapping and structural interpretation in south-west Iran, Zagros Structural Belt. *International Journal of Remote Sensing* 25, 4715-4727.
- Bannert, D., Cheema, A., Ahmed, A., Schäffer, U., 1993. The Structural Development of the Western Fold Belt, -Pakistan. *Geologisches Jahrbuch., Reihe B.*
- Beauchemin, M., Fung, K.B., 2001. On statistical band selection for image visual izati on. *PE & RS-Photogrammetric Engineering and Remote Sensing* 67,571-574.
- Bilotti, F., Shaw, J.H., Brennan, P.A., 2000. Quantitative structural analysis with stereoscopic remote sensing imagery. *AAPG bulletin* 84, 727-740.

- Bossart, P., Dietrich, D., Greco, A., Ottiger, R., Ramsay, J.G., 1988. The tectonic structure of the Hazara- Kashmir Syntaxis, southern Himalayas, Pakistan. *Tectonics* 7, 273-297.
- Chavez, P., Sides, S.C., Anderson, J.A., 1991. Comparison of three different methods to merge multiresolution and multispectral data- Landsat TM and SPOT panchromatic. *Photogrammetric Engineering and remote sensing* 57, 295-303.
- Clark, R.N., 1999. Spectroscopy of rocks and minerals, and principles of spectroscopy. *Manual of remote sensing* 3, 3-58.
- Clark, R.N., King, T.V., Klejwa, M., Swayze, G.A., Vergo, N., 1990. High spectral resolution reflectance spectroscopy of minerals. *Journal of Geophysical Research: Solid Earth* (19782012) 95, 12653-12680.
- Crippen, R., Hajic, E., Estes, J., Blom, R., 1990. Statistical band and band-ratio selection to maximize spectral information in color composite displays. *Remote Sensing of Environment*, (submitted).
- Dehnavi, A.G., Sarikhani, R., Nagaraju, D., 2010. Image processing and analysis of mapping alteration zones in environmental research, East of Kurdistan, Iran. *World Applied Sciences Journal* 11, 278-283
- DiPietro, J.A., Pogue, K.R., 2004. Tectonostratigraphic subdivisions of the Himalaya: a view from the west. *Tectonics* 23.
- Dogan, H., 2008. Applications of remote sensing and Geographic Information Systems to assess ferrous minerals and iron oxide of Tokat province in Turkey. *International Journal of Remote Sensing* 29, 221-233.
- Eardley, A.J., 1942. Aerial photographs: their use and interpretation. *Aerial photographs: their use and interpretation*.
- Ferrero, A., Forlani, G., Roncella, R., Voyat, H., 2009. Advanced geostructural survey methods applied to rock mass characterization. *Rock mechanics and rock engineering* 42, 631-665.
- Ferrero, A.M., Migliazza, M., Roncella, R., Rabbi, E., 2011. Rock slopes risk assessment based on advanced geostructural survey techniques. *Landslides* 8, 221-231.
- Gad, S., Kusky, T., 2006. Lithological mapping in the Eastern Desert of Egypt, the Barramiya area, using Landsat thematic mapper (TM). *Journal of African Earth Sciences* 44, 196-202.
- Gaffey, S.J., 1986. Spectral reflectance of carbonate minerals in the visible and near infrared (0.35-2.55 microns); calcite, aragonite, and dolomite. *American Mineralogist* 71, 151-162.
- Goetz, A.F., Rowan, L.C., 1981. Geologic remote sensing. *Science* 211, 781-791.

- Hunt, G.R., Salisbury, J.W., 1971. Visible and near infrared spectra of minerals and rocks. II. Carbonates. *Modern Geology* 2, 23-30.
- Imbroane, A., Melenti, C., Gorgan, D., 2007. Mineral Explorations by Landsat Image Ratios, Symbolic and Numeric Algorithms for Scientific Computing, 2007.SYNASC. International Symposium on. IEEE, pp. 335-340.
- Jones, A., 1961. Reconnaissance geology of part of West Pakistan. A Colombo Plan Cooperative Project. Toronto, Canada: Government of Canada.
- Kavak, K., 2005. Determination of palaeotectonic and neotectonic features around the Menderes Massif and the Gediz Graben (western Turkey) using Landsat TM image. *International Journal of Remote Sensing* 26, 59-78.
- Kavak, K., Inan, S., 2002. Enhancement facilities of SPOT XS imagery in remote sensing geology: an example from the Sivas Tertiary Basin (central Anatolia/Turkey). *International Journal of Remote Sensing* 23, 701-710
- Kaya, Ş., Müftüođlu, O., Tüysüz, O., 2004. Tracing the geometry of an active fault using remote sensing and digital elevation model: Ganos segment, North Anatolian Fault zone, Turkey. *International Journal of Remote Sensing* 25, 3843-3855
- Kottenstette, J., 2005. Measurement of geologic features using close range terrestrial photogrammetry, Alaska Rocks 2005, The 40th US Symposium on Rock Mechanics (USRMS). American Rock Mechanics Association.
- Latif, M., 1970. Explanatory notes on the geology of southeastern Hazara to accompany the revised geological map. *Jahrb. Geol. Bundesanst* 15, 5-20.
- Mars, J.C., Rowan, L.C., 2010. Spectral assessment of new ASTER SWIR surface reflectance data products for spectroscopic mapping of rocks and minerals. *Remote Sensing of Environment* 114, 2011-2025.
- MORRIS, R.H., 1964. PROCEDURES AND STUDIES IN PHOTO GEOLOGY. *Bulletin-United States Geological Survey* 1043.
- Paine, D.P., Kiser, J.D., 2012. Aerial photography and image interpretation. John Wiley & Sons.
- Qasim, M., Khan, M.A., Haneef, M., 2014. Stratigraphic characterization of the Early Cambrian Abbottabad Formation in the Sherwan area, Hazara region, N.Pakistan: Implications for Early Paleozoic stratigraphic correlation in NW Himalayas, Pakistan. *Journal of Himalayan Earth Sciences* Volume 47, 25-40.
- Qasim, M., Khan, M.A., Haneef, M., 2015. Stratigraphic characterization and



- structural analysis of the northwestern Hazara Ranges across Panjal Thrust, northern Pakistan. *Arabian Journal of Geosciences*, 1-19.
- Rajendran, S., Thirunavukkarasu, A., Balamurugan, G., Shankar, K., 2011. Discrimination of iron ore deposits of granulite terrain of Southern Peninsular India using ASTER data. *Journal of Asian Earth Sciences* 41, 99-106.
- Rawashdeh, S.A., Saleh, B., Hamzah, M., 2006. The use of remote sensing technology in geological investigation and mineral detection in El Azraq-Jordan. *Cybergeo: European Journal of Geography*.
- Sabins, F.F., 1999. Remote sensing for mineral exploration. *Ore Geology Reviews* 14, 157-183.
- Schetselaar, E.M., Chung, C.-J.F., Kim, K.E., 2000. Integration of Landsat TM, Gamma-Ray, Magnetic, and Field Data to Discriminate Lithological Units in Vegetated. *Remote Sensing of Environment* 71, 89-105.
- Vincent, R.K., 1997. *Fundamentals of geological and environmental remote sensing*. Prentice Hall Upper Saddle River, NJ.
- Wadia, D., 1931. The syntaxis of the northwest Himalaya: its rocks, tectonics and orogeny. *Rec. Geol. Surv. India* 65, 189-220.
- Yamaguchi, Y., Kahle, A.B., Tsu, H., Kawakami, T., Pniel, M., 1998. Overview of advanced spaceborne thermal emission and reflection radiometer (ASTER). *Geoscience and Remote Sensing, IEEE Transaction on* 36, 1062-1071.
- Yazdi, M., Taheri, M., Navi, P., Sadati, N., 2013. Landsat ETM+ imaging for mineral potential mapping: application to Avaj area, Qazvin, Iran. *International journal of remote sensing* 34, 5778-5795.
- Yesou, H., Besnus, Y., Rolet, J., 1993. Extraction of spectral information from Landsat TM data and merger with SPOT panchromatic imagery: contribution to the study of geological structures. *ISPRS Journal of Photogrammetry and Remote Sensing* 48, 23-36.